

The origin of the most recently ejected OB runaway star from the R136 cluster

Simon Portegies Zwart

*Leiden Observatory, Leiden University, PO Box 9513, 2300 RA, Leiden, The Netherlands.**

Mitchel Stoop

*Anton Pannekoek Institute for Astronomy, University of Amsterdam,
Science Park 904, Amsterdam, 1098 XH, the Netherlands.*

Lex Kaper, Alex de Koter,[†] and Steven Rieder[†]

*Anton Pannekoek Institute for Astronomy, University of Amsterdam,
Science Park 904, Amsterdam, 1098 XH, the Netherlands*

Tomer Shenar

*Departamento de Astrofísica, Centro de Astrobiología (CSIC-INTA),
Ctra. Torrejón a Ajalvir km 4, 28850 Torrejón de Ardoz, Spain.*

(Dated: July 17, 2025)

The $\sim 60\,000$ solar-mass (M_\odot) star-cluster R136 (NGC 2070) in the Tarantula Nebula in the Large Magellanic Cloud is the host of at least 55 massive stars ($M \gtrsim 10\,M_\odot$) which move away from the cluster at projected velocities ≥ 27.5 km/s [1]. The origin of the high velocities of such runaway stars have been debated since the 1960s, resulting either from dynamical ejections [2, 3] or from supernova explosions [4]. Due to the Gaia satellite’s outstanding precision, we can now retrace the most recently ejected binary star, Mel 34, back to the center of R136 and reconstruct the events that 52 000 years ago led to its removal from R136, i.e., we establish its dynamical interaction and ejection history. We find that this ejection requires the participation of 5 stars in a strong interaction between a triple composed of the tight massive binary Mel 39 orbited by the star VFTS 590, and the binary star Mel 34. The participation of 5 stars is unexpected because runaway stars were not expected to result from triple interactions [5]. The deterministic nature of the Newtonian dynamics in the scattering enables us to reconstruct the encounter that ejected Mel 34. We then predict that Mel 39 is a binary star with an $80\,M_\odot$ companion star that orbits within $\sim 1^\circ$ in the same plane as Mel 34, and escapes the cluster with a velocity of ~ 64 km/s. The five stars will undergo supernova explosions in the coming 5 Myr at a distance of ~ 180 pc to ~ 332 pc from their birth location (R 136). The resulting black hole binaries, however, are not expected to merge within a Hubble time.

1. INTRODUCTION

The young ($\lesssim 1$ Myr) and massive ($\sim 60\,000\,M_\odot$) star cluster NGC2070 (also known as R136) in the Large Magellanic cloud is one of the most dynamically active regions in the local group [6]. It is host of the largest known population of stars more massive than $100\,M_\odot$ and several even in excess of $150\,M_\odot$ [7, 8].

With a core-density of $n \simeq 4.2 \times 10^5$ stars/pc³, and a mean stellar mass of $\langle m \rangle \sim 3.6\,M_\odot$ in the segregated core of R136, stellar encounters are common and violent, leading to frequent stellar collisions [9] and high-velocity ejections [5]. Stoop et al (2024) reported on 20 stars of $\gtrsim 10\,M_\odot$ escaping the cluster with a velocity of > 27.5 km/s in the last 0.84 Myr, leading to a mean ejection rate of $\Gamma \gtrsim 24\,\text{Myr}^{-1}$.

These runaways cannot have been produced in the supernova explosion in close binary systems [2, 3] because with an age of 1.5–2 Myr [1] the cluster is too young for the first supernova to occur. These observed runaway stars must then have been violently ejected in multi-body encounters [10, 11] or in the kinematically cold collapse in a multi-clump cluster merger [12]. The latter process explains about half the runaways ejected in the recent wave, particularly those in a preferred direction and with velocities around 40 km/s, as discussed in [1, 12].

The most recently ejected runaway binary Mel 34 is moving too fast to be ejected through a multi-clump cluster merger, and must have been ejected in a strong encounter with other stars. Here, we present a forensic analysis of the last encounter that led to the dynamical ejection of Mel 34. We reconstruct the details of this encounter and identify the participating other stars, which were ejected in the same event.

2. THE LAST MASSIVE RUNAWAY STAR MEL 34

The most recently ejected object is the binary Mel 34AB composed of two stars of $139^{+21}_{-18}\,M_\odot$ and $127 \pm 17\,M_\odot$ in an eccentric ($e = 0.68 \pm 0.02$) 154.55 ± 0.05 day ($a \simeq 3.63$ au) orbit. Mel 34 was ejected 52 ± 8 kyr ago with a projected velocity

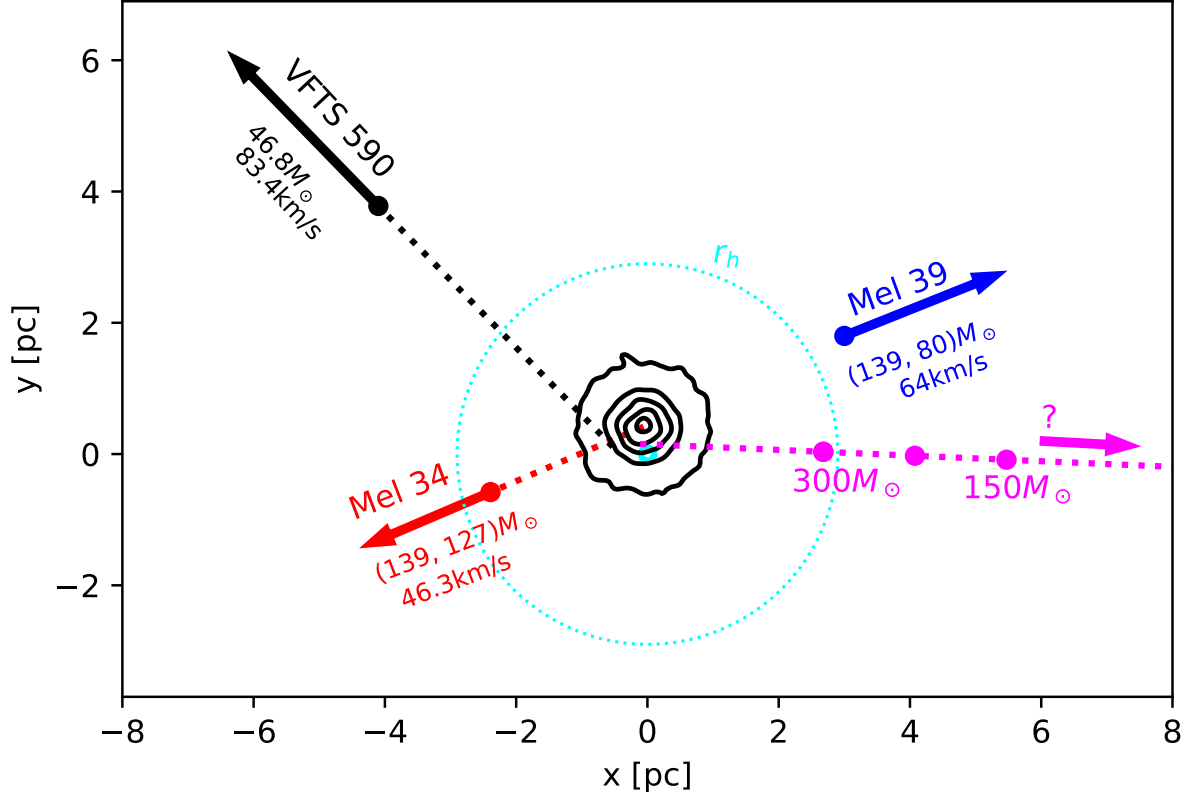


FIG. 1. Reconstruction of the historic trajectory for the massive binary Mel 34 (red), VFTS 590 (black) and the mystery runaway star that would conserve angular momentum in a binary-binary encounter (magenta). The arrows are proportional to the velocities (except the magenta one, which is mass-dependent). The cyan-colored circles indicate the cluster's core and half-mass radii. The contours give the probability density distribution for the encounter site at 0.01, 0.2, 0.4, etc. confidence levels. The blue dot to the right indicates where Mel 39 is observed, the arrow shows our predicted velocity vector.

of $\sim 46.3 \pm 6.4$ km/s [13].

The characteristics of Mel 34 are surprisingly consistent with a dynamically formed binary [14]: the system exhibits a tight orbit with high eccentricity, and both stars are among the most massive in the cluster. In addition, tracing back Mel 34's trajectory, it passed 0.046 to 0.060 Myr ago to within the projected position of $(-0.058 \pm 0.65, 0.42 \pm 0.28)$ pc from the estimated center of R136 [1], as depicted in fig. 1.

3. THE BALLISTICS OF THE LAST RUNAWAYS

Ejecting a massive binary with such a high velocity requires an unusually strong encounter with other stars. The binary itself can deliver enough energy for such an ejection if the encountering star is of comparable mass, but can we identify this other star?

Mel 34 may have formed as a wide binary system, over time decreasing its orbital separation [a process called hardening, 15] through interactions with its cluster siblings and ambient gas. At orbital separations less than $a \sim 1400$ au its binding energy would exceed $E_{\text{bin}} \gtrsim 10$ kT (see appendix appendix B, on the use of kT as a unit of energy). At a ~ 60 au (~ 600 kT) interactions become sufficiently energetic for ejecting other stars. From that moment, such a binary is referred to as a bully binary. These bully binaries play a prominent role in the dynamical evolution of stellar clusters [5]. Although not currently a cluster member, Mel 34 today has an equivalent binding energy of $E_{\text{bin}} \sim 4300$ kT, making it a bully binary.

The typical energy release in an encounter between a target bully binary (with mass m_t) and a projectile star with mass m_p is [16]

$$dE_{\text{bin}} = \xi q E_{\text{bin}}. \quad (1)$$

Here $q \equiv m_p/m_t$, and $\xi = \mathcal{O}(0.2)$ (a dimension-less scaling factor depending on equipartition [see 15, eqs. 4.29 and 5.40], although the precise value depends on the details of the encounter). A bully binary leads to roughly 8 escapers of comparable mass before it is sufficiently hard to eject itself [17]. When Mel 34 ejected itself in a dynamical interaction in R136's core, the encountering object being lower in mass was also ejected because linear momentum in such interactions is conserved.

The $46.8^{+6.5}_{-6.1} M_\odot$ star VFTS 590 was ejected 62^{+5}_{-4} kyr ago from $(-0.47, 0.31)$ pc relative to the cluster center with a velocity of 83.4 ± 6.2 km/s (~ 324 kT, see also figure 1) [1]. Both stars, Mel 34 and VFTS 590, are then ejected at the same time within 1.1 standard deviations. VFTS 590 was launched in a direction almost perpendicular to the bulk of the other recently ejected stars, suggesting that it does not belong to the population of runaways accelerated in the kinematically cold sub-cluster merger. However, the amount of kinetic energy required to eject Mel 34 and VFTS 590 exceeds ~ 891 kT; more than 8 times the expected $dE_{\text{bin}} \sim 107$ kT generated in such an encounter (see eq. (1)).

The alternative exchange interaction in which, for example, VFTS 590 is the original secondary in a binary with Mel 34B, can deliver the appropriate amount of energy, but to account for the kinetic energy of the two runaways and Mel 34's binding energy, the pre-encounter orbital separation of the binary should be between 0.8 au and 3 au. Such an interaction typically has a 17 times higher probability to result in a collision between two or more stars rather than a clean exchange. The latter cross section is only $\sigma \sim 11 \text{ au}^2$, or equivalently expressed in the encounter rate $\Gamma \sim 83 \text{ Myr}^{-1}$, and the typical velocity with which VFTS 590 would be ejected is much too high (up to ~ 140 km/s). VFTS 590, however, cannot have been responsible for the ejection of Mel 34 because the interaction does not conserve angular momentum (see appendix C).

4. THE OTHER STARS PARTICIPATING IN THE ENCOUNTER

Angular momentum can only be conserved if at least one other star participated in the encounter, which would also have been ejected from the cluster (fig. 1). We performed 4-body (binary-binary, and triple-single) scattering experiments to determine the most favorable mass of the unknown runaway (see appendix E). The largest cross-section and consistent post-encounter parameters are achieved for a $90 \pm 3 M_\odot$ star: which would be VFTS 590's binary companion before the encounter (see appendix D). This mystery runaway star would now be at a distance of about 8.5 ± 0.3 pc from R136's center. In fig. 1, we show the escaping star's trajectory that conserves linear momentum. There is no prominent candidate star with a measured proper motion along this trajectory up to a distance of ~ 600 pc [1], although it could be obscured, or below the detection limit (of $\sim 10 M_\odot$ for a main-sequence star). We consider the possibility that Mel 34 was ejection through the interaction with an intermediate-mass black hole exotic because the cluster is insufficiently dense and too young to have formed such an object [18].

Almost directly opposite Mel 34 at the other side of the core of R 136, at an angle of $\sim 179.8^\circ$, another binary called Mel 39 runs away from R 136. The Wolf-Rayet primary star in Mel 39 is $\sim 140 M_\odot$. An orbital period of about 92 days is reported, but the companion star is not yet identified [19].

Mel 39 is about 20% further away (in projection) from the center of R 136 than Mel 34 (see fig. A.I). If both objects ejected each other from the cluster center, the projected velocity for Mel 39 would be about 64 km/s. With the conservation of linear momentum, we estimate the total mass of Mel 39 $\sim 220 M_\odot$; that leaves about $80 M_\odot$ for its companion star. Interestingly, this is consistent with the spectroscopically determined mass of $80 \pm 11 M_\odot$, derived by [20]. It is conceivable that such a secondary was not observed in optical surveys because the primary apparently outshines it. With these parameters, its orbital separation will be about 2.48 au, somewhat tighter than Mel 34, but with a binding energy of ~ 4000 kT, it is softer.

A single star (VFTS 590) that simultaneously engaged two binaries in a strong encounter is improbable and leads to too high runaway speeds except if the relative encounter-velocity $\gtrsim 15$ km/s (see appendix A). The latter exceeds the cluster's escape speed, making such an encounter highly unlikely. The star VFTS 590 then must have orbited one of the interacting binaries.

5. RECONSTRUCTING THE INTERACTION

Exploring the entire parameter space of a 5-body encounter is hindered by its large volume. We can limit the available parameter space enormously by requirements that energy, and momentum (linear and angular) are conserved throughout the interaction.

The two binaries, currently with binding energies of ~ 4300 kT and ~ 4000 kT for Mel 34 and Mel 39, respectively, have to generate enough energy to accelerate VFTS 590 (324 kT), Mel 34 (567 kT), and Mel 39 (896 kT) to their present-day velocities. This total of 1787 kT has to come from the binding energies of the binary and the triple. Note that for an equal-mass encounter, the delivery of 1787 kT can satisfactorily be achieved by two binaries with a total binding energy of ~ 8935 kT, which is only slightly higher than the total binding energy in today's two binaries, leaving roughly 635 kT for the orbit of the tertiary. We then argue that the binding energies of the two binaries is rather well constrained, and we only have to identify the various

id	initial configuration	σ [10^6 au^2]	$f_{\text{esc, VFTS590}}$	f_{run}	$\Gamma_{\text{esc, VFTS590}}$ Myr $^{-1}$
A	$\langle((t_{11}, t_{12}), t_2), (\text{Mel39B}, \text{VFTS 590})\rangle$	61.8	0.002	0.000	0.0
B	$\langle((t_{11}, t_{12}), \text{VFTS 590}), (p_1, \text{Mel39B})\rangle$	53.5	0.397	0.016	6.2
C	$\langle((t_{11}, t_{12}), \text{Mel39B}), (p_1, \text{VFTS 590})\rangle$	38.6	0.002	0.000	0.0
D	$\langle((t_{11}, \text{VFTS 590}), t_2), (p_1, \text{Mel39B})\rangle$	90.5	0.129	0.002	1.1
E	$\langle((t_{11}, \text{Mel39B}), t_2), (p_1, \text{VFTS 590})\rangle$	63.0	0.004	0.000	0.0
F	$\langle((t_{11}, \text{VFTS 590}), \text{Mel39B}), (p_1, p_2)\rangle$	106	0.099	0.007	5.2
G	$\langle((t_{11}, \text{Mel39B}), \text{VFTS 590}), (p_1, p_2)\rangle$	101	0.442	0.049	34.9
H	$\langle((\text{Mel39B}, \text{VFTS 590}), t_2), (p_1, p_2)\rangle$	109	0.109	0.006	4.6

TABLE 1. The 8 initial configurations for a triple-binary encounter. The target triple has an inner separation $a_{\text{in}} = 4 \text{ au}$, and outer separation $a_{\text{out}} = 40 \text{ au}$. The projectile binary with $a_p = 6 \text{ au}$, encounters the target triple with a relative velocity of $v_{\text{enc}} = 7 \text{ km/s}$. The last four columns give the interaction cross-section (σ), the fraction of cases in which VFTS 590 is ejected ($f_{\text{esc, VFTS590}}$), with a velocity of at least $v_{\text{ej}} \gtrsim 27.6 \text{ km/s}$ (f_{run}), and the corresponding rate that VFTS 590 and the two surviving binaries are ejected with at least $v_{\text{ej}} \gtrsim 27.6 \text{ km/s}$ calculated for the core collapsed cluster R136 ($\Gamma_{\text{esc, VFTS590}}$). The most likely scenario is G.

components. Note that the minimal stable orbit for VFTS 590 as tertiary component around Mel 34 or Mel 39 has a semi-major axis of $\sim 25.1 \text{ au}$ or 36.6 au , respectively [21]. The binding energy of these orbits corresponds to 300 kT and 362 kT, respectively.

To simplify the discussion, we parametrize the interaction as a target triple t with inner components t_{11} and t_{12} , and outer component t_2 . The projectile binary comprises two stars p_1 and p_2 . We then write the pre-encounter topology as $\langle((t_{11}, t_{12}), t_2), (p_1, p_2)\rangle$. Here, the angle brackets indicate a hard dynamical encounter, and parenthesis the bound pairs.

The various stars can be divided into a triple and a binary in 5! combinations. We reduce parameter space by adopting the masses of VFTS 590 ($50 M_{\odot}$) and Mel 39B ($80 M_{\odot}$) unique, and assuming $130 M_{\odot}$ for Mel 34A, Mel 34B, and Mel 39A. We further adopted circular orbits for the projectile binary and the inner binary of the target triple. Relaxing this assumption does not affect the energetics of the encounter. Although, we cannot exclude that Mel 34 has some residual eccentricity from a previous encounter, the tidal circularization time scale for Mel 39 is smaller than its lifetime [see Eq. 4.13 of 22], and it was probably circularized before the encounter. The eccentricity of the tertiary was taken randomly from the thermal distribution with the requirement of a stable triple (see table 1).

We then constrain the pre-encounter parameters by determining the most probable configuration, and in addition to that, identify which of the 5 component should be associated with VFTS 590 or Mel 39B. The resulting 8 combinations are listed in table 1 as scenario A till H (see also appendix E).

The optimal parameters are determined by running 5-body simulations to reproduce the post-encounter binaries, Mel 34 and Mel 39, with their appropriate orbital separations of 3.63 au and 2.48 au, respectively and runaway speeds (see appendix E). With an interaction rate of 34.9 Myr^{-1} , we favor scenario G. VFTS 590 then identifies with t_2 , the tertiary orbiting a binary, with Mel 39B as the secondary (t_{12}). The presented calculations assume an orbital separation of 4 au for the inner (target) binary of the triple (t_{11}, t_{12}), 40 au (up to 200 au) for the outer orbit, and 6 au for the projectile binary (p_1, p_2).

To further identify the three remaining stars, t_{11} , p_1 and p_2 , we calculate the relative frequency for each of the various configurations for the interactions in scenarios G (table E.I in appendix E lists all relative probabilities for scenarios A till H).

The binary-preserving encounters for model G have the largest probability with a rate of $\sim 27 \text{ Myr}^{-1}$; conveniently close to the observed 24 Myr^{-1} . The most probable interaction then is

$$\langle((\text{Mel39A}, \text{Mel39B}), \text{VFTS590}), (\text{Mel34A}, \text{Mel34B})\rangle \rightarrow (\text{Mel34A}, \text{Mel34B}), (\text{Mel39A}, \text{Mel39B}), \text{VFTS590} \quad (2)$$

The interaction

$$\langle((\text{Mel34A}, \text{Mel39A}), \text{VFTS590}), (\text{Mel34B}, \text{Mel39B})\rangle \rightarrow \dots \quad (3)$$

leading to the same final configuration is less probably by a factor ~ 5 ($\Gamma \simeq 6 \text{ Myr}^{-1}$).

Figure 2 presents an example encounter showing interaction G. The cross section is largest for orbital separations of the inner target and projectile binaries of 4 au and 6 au, respectively, and these reproduce the current observed orbital separations and runaway velocities. The orbital separation of VFTS 590 around Mel 39 (in the range of 40 au to 200 au) has a negligible effect on the interaction cross-section because the energetics of the interaction is dominated by the binding energies of the two binaries (see appendix E).

Changing the incoming relative encounter velocity affects the result as expected through gravitational focusing. We prefer a relative encounter velocity of 7 km/s because it is consistent with the cluster's core velocity dispersion and the resulting cross-section is consistent with the estimated encounter rate for the cluster center (see appendix E).

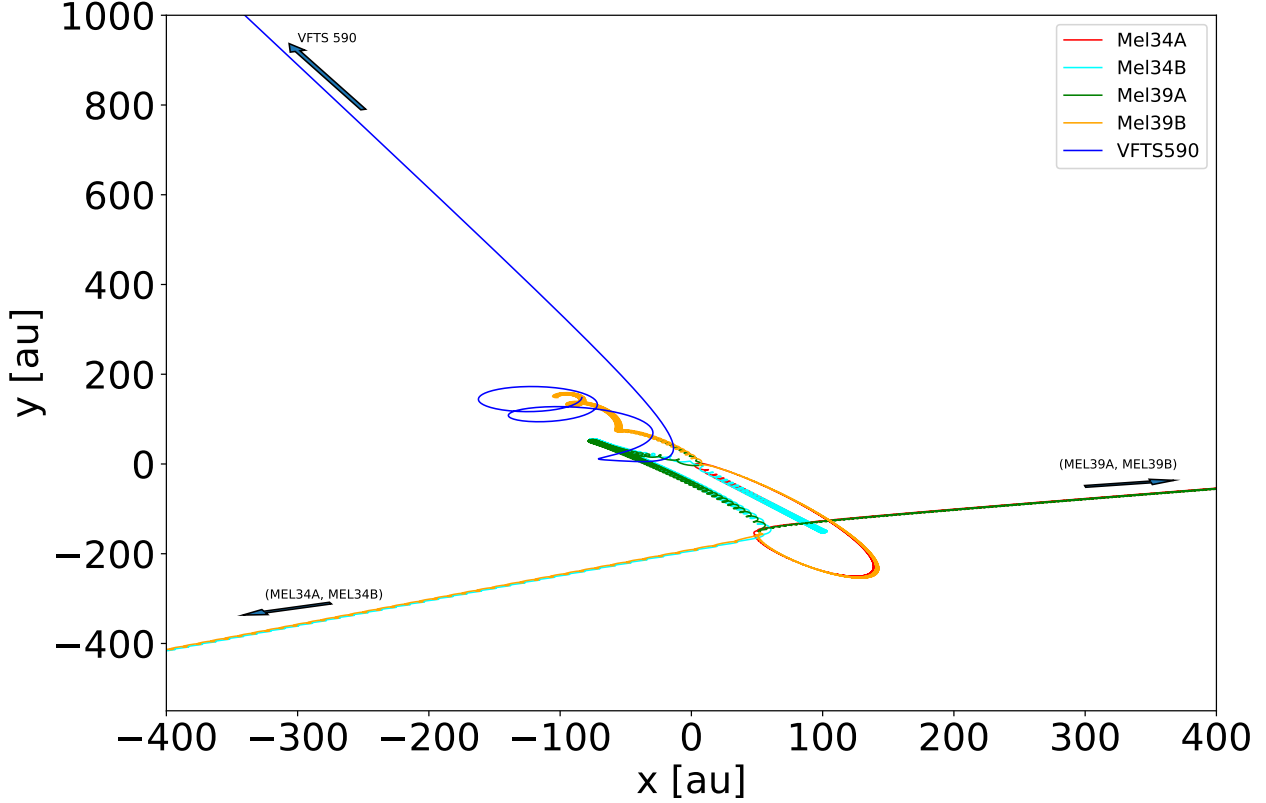


FIG. 2. Interaction between the triple ((Mel 34A, Mel 39B), VFTS 590) and the binary (Mel39A, Mel34B) for scenario B in a strong dynamical interaction with a relative velocity of 7 km/s. The interaction leads to the ejection of VFTS 590 as a single star, and the preservation of the two binaries. The two escaping binaries are ejected in opposite directions, consistent with the observations, including the ejection velocities, the relative orbital separations and the eccentricity of Mel 34.

6. RESULTS

The last energetic encounter in R 136 occurred $\sim 52\,000$ years ago between a hierarchical triple and a binary. The triple was composed of ((Mel 39A, Mel 39B), VFTS 590) with orbital separations of 4.0 ± 0.5 au for the inner target orbit, and an outer orbit between 40 au and 200 au. Before the encounter, the binary (Mel 34A, Mel 34B) had an orbital separation of 6.0 ± 0.5 au.

The interaction reproduces statistically the observed orbital separations of Mel 34 and Mel 39, the velocities of both binaries, and the observed velocity of VFTS 590. Table 2 presents the pre- and post-encounter parameters. In figure 3 we present the distribution of semi-major axis and eccentricity for the post-encounter binaries Mel 34 (shades) and Mel 39 (contours). The orbital separations for both binaries are well constrained by the simulations and match the observed values. The relatively small dispersion in probability density distribution for the eccentricities comes as a surprise, as we naively would have expected a close-to-thermal distribution.

In our best solution Mel 39A is accompanied by an $80\,M_{\odot}$ star in a 2.48 au orbit. The interaction between the two binaries induced a high eccentricity ($e = 0.78 \pm 0.09$ but with a median of 0.73 ± 0.02) in Mel 39, and a mean runaway velocity $v_{\text{run}} = 70.6 \pm 8.6$ (median is 60.7 km/s). The two binaries are ejected in almost opposite directions with a median angle of $\Theta \simeq 172^{\circ}$ ($\langle \Theta \rangle = (152.9 \pm 24.2)^{\circ}$). The relative inclination between Mel 34 and Mel 39 is $\delta i = (-1.1 \pm 56)^{\circ}$. Our derived inclination for Mel 39 is consistent with the recent observed value of 90° [20] and comparable to their observed eccentricity of 0.618 ± 0.014 . But [20] arrive at a somewhat wider orbit. The argument of pericenter and the line of the ascending node do not show any systematic correlations in the simulation results.

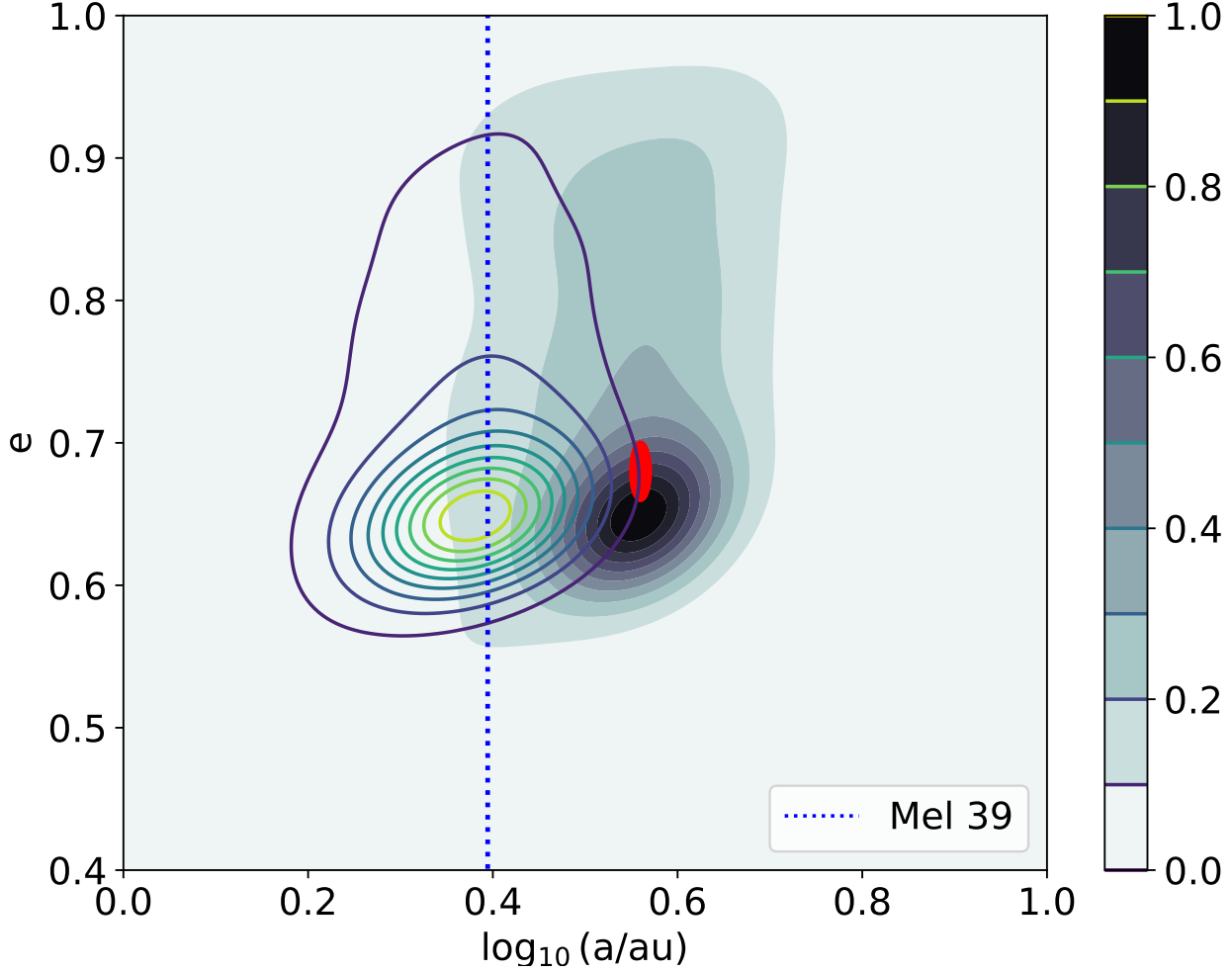


FIG. 3. Orbital separation vs eccentricity for Mel34 (gray shades, see color-bar to the right) and Mel39 (contours, overplotted in the colorbar). The two distributions are generated from the preserving interaction with an initial separation of 4 au for Mel39, 40 au for VFTS 590 around Mel 39, and 6 au for Mel 34. The red ellipsoid point gives the observed orbital elements for Mel 34 (its size is 2 standard deviations), and the vertical blue dotted line gives the observed semi-major axis (assuming an $80 M_{\odot}$ star for the secondary) for Mel 39.

Binary	Tertiary	a_{init} [au]	a_{fin} [au]	e_{fin}	v_{run} km/s
((Mel39A Mel39B)		4	1.39 ± 0.57	0.84 ± 0.10	58.7 ± 3.8
	VFTS 590)	40 – 200			65.1 ± 9.2
(Mel34A Mel34B)		6	6.03 ± 9.14	0.74 ± 0.08	70.6 ± 8.6

TABLE 2. Pre and post-encounter orbital parameters for the two binaries and the tertiary component. The first row identifies the binary components followed by the name of the third star. The subsequent column gives the initial orbital separation (a_{init}). The last three columns give the final semi-major axis (a_{fin}), eccentricity (e_{fin}) and the mean ejection velocity (with respect to the barycenter, v_{run}).

7. DISCUSSION AND CONCLUSIONS

The two bully binaries can deliver sufficient energy to eject all the 20 observed runaways of $\gtrsim 10 M_{\odot}$ in the last 0.84 Myr. The asymmetry in the direction of the recent runaways [1], however, suggests that about half of them was ejected in a cold sub-cluster merger, as discussed in [12]. Considering the top-heavy mass function and the hardness of the two bullies (2470 kT for Mel 39, and 2230 kT for Mel 34), we then expect that ~ 52 more runaways will be discovered with a mass between $1 M_{\odot}$ and the observational detection limit of $\sim 10 M_{\odot}$; with early ejected runaways having systematically lower velocities.

Both bully binaries ran into each other about 52 000 years ago, leading to their mutual ejection; this epoch of bully binaries has now temporarily ceased. Mel 34 and Mel 39 may have prevented the early hardening (from ~ 10 kT to 1000 kT) of a new bully, and it may take a while before another binary takes their place. The four binaries R136 38, R136 39 (not to be confused with Mel 39), R136 42, and R136 77 [23] have such short orbital periods that a strong interaction is expected to lead to a collision rather than a dynamical ejection.

In about 3 Myr, both binaries Mel 34 and Mel 39 will circularize, experience mass transfer, and eventually, after about 5 Myr, the stars explode in supernovae. By that time Mel 34 has traveled ~ 184 pc, and Mel 39 ~ 258 pc. Mel 34 and Mel 39 are the prototypical example binaries that eventually lead to black-hole mergers [24], though not in a Hubble time.

We demonstrated how observing the physical properties of runaway stars provides the opportunity to reconstruct in detail the dynamical history of young-massive stellar clusters.

DATA AND CODE AVAILABILITY

All data is available at zenodo <https://zenodo.org/uploads/10256841> under DOI: 10.5281/zenodo.10256841, and all the source code is on github <https://github.com/amusecode/Starlab>.

Appendix

To reconstruct the last encounter that ejected Mel 34 from the star cluster NGC2070 (R136), we performed more than 2 million scattering experiments for 3, 4 and 5 bodies, 12 full N-body simulations of the entire star cluster, 5 single stellar-evolution calculations, and 2 binary-evolution calculations. In all simulations, we adopt the zero-age main-sequence radii of the stars calculated using the AMUSE stellar_simple.py script [25]. The radii for Mel34A, Mel34B, and Mel 39A are then $\sim 17 R_{\odot}$ [13]. The two stars Mel 39B and VFTS 590 are $15 R_{\odot}$ and $11 R_{\odot}$, respectively.

Appendix A: The cluster R136

The stars in a cluster are usually distributed with a power-law mass-function with a slope of -2.35 between the hydrogen-burning limit (of about $0.08 M_{\odot}$) and some maximum mass (of $\sim 100 M_{\odot}$). This typical mass function has a mean mass of $\sim 0.35 M_{\odot}$ [26], but the core population of a collapsed cluster is considerably more massive. We numerically explore the core-mass function of a $60\,000 M_{\odot}$ non-mass segregated and relatively cold ($Q = 0.1$ to virializd $Q \equiv E_{\text{kin}}/E_{\text{pot}} = 0.5$) Plummer [27] sphere with a half-mass radius of 2.9 pc. Most simulated clusters virialize within ~ 0.2 Myr, at which point, the core has shrunk to ~ 0.10 pc [28]. By this time, the mean mass within 0.06 pc is about $11 M_{\odot}$ (with an average of $\sim 3.6 M_{\odot}$ in the core). At this time the density in the cluster core $n \simeq 4.2 \times 10^5$ stars/pc³, and $\rho \simeq 1.5 \times 10^6 M_{\odot}$ /pc³.

The typical ejected star will follow the top-heavy core mass function [5]. In figure A.I, we compare the top-heavy mass function of the recent runaways with the Salpeter slope.

With a core radius of $r_{\text{core}} \simeq 0.1$ pc, and a half-mass radius of 2.9 pc, the cluster NGC2070 (or R136) resembles a King profile with a dimensionless depth of the central potential of $W_0 \sim 9.8$ [29]. Such a King model has a relative core mass of 0.017, or $\sim 10^3 M_{\odot}$ and a velocity dispersion of ~ 7 km/s. As a consequence, R136 is in a state of gravothermal collapse [30], and prone to strong dynamical interactions.

Appendix B: Soft and Hard binaries

To mediate the discussion, it helps to consider the cluster as a gas and define the unit of energy in terms of $\text{kT} \propto mv^2$ as the kinetic encounter energy between stars in the cluster core [16]. With a mean stellar mass in the cluster core of $3.9 M_{\odot}$ to $11.0 M_{\odot}$ (see appendix A), the core's kinematic unit for energy $1 \text{ kT} \simeq 1.1 \cdot 10^{46}$ erg. For convenience we adopt as definition for $E_{\text{kT}} \equiv 10^{46}$ erg.

The binding energy of a binary with orbital separation a and two stars of masses M and m is

$$E_{\text{bin}} = \frac{GMm}{2a} \quad (\text{B.I})$$

A binary is generally considered hard once it's binding energy exceeds 10kT. Mel 34, residing in the cluster core would be hard at an orbital separation of about 1400 au.

Ejecting a $10 M_{\odot}$ star from R 136 with a velocity of 27.5 km/s would require a total kinetic energy of ~ 6.8 kT. Mel 34 can generate this much energy in an encounter if it has a binding energy of $E_{\text{bin}} \gtrsim 910$ kT (see eq. (1) in the main paper), or an

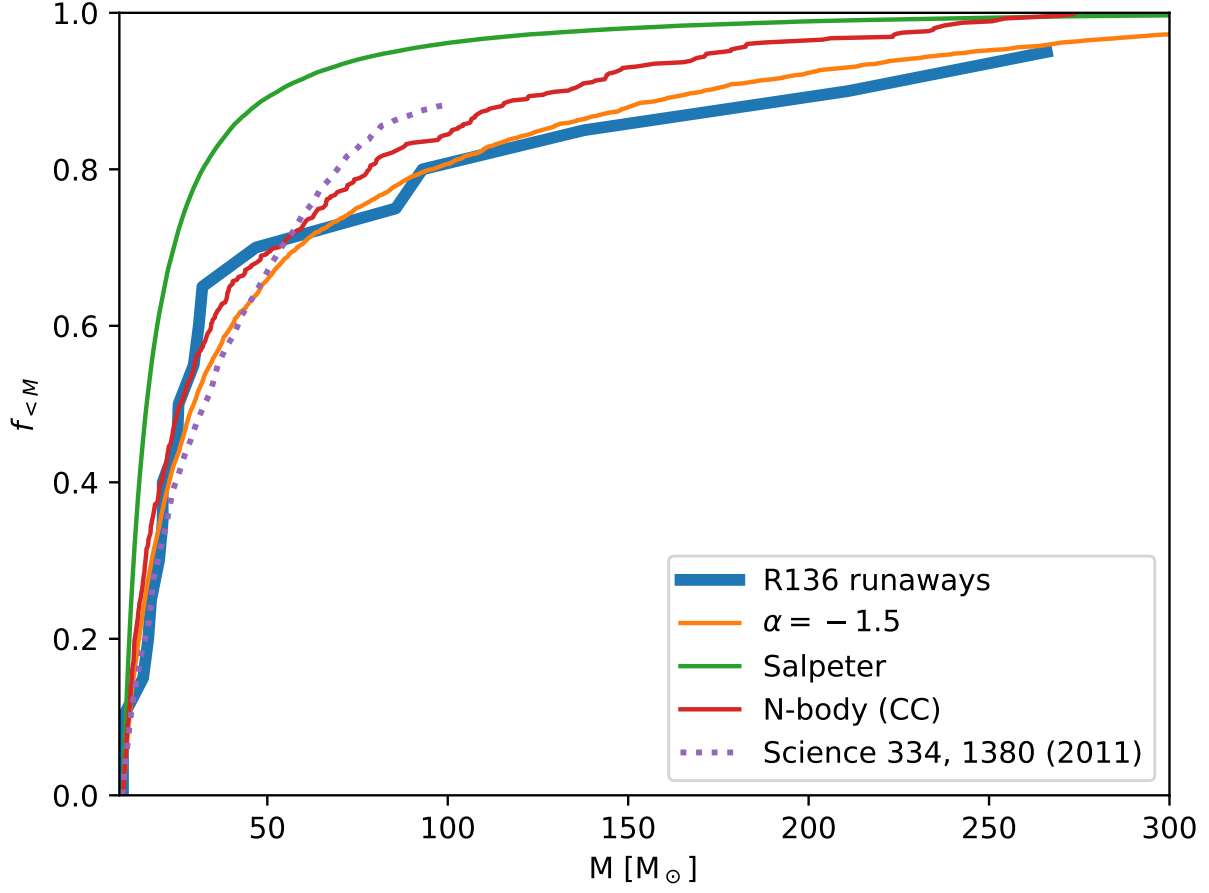


FIG. A.I. cumulative distribution of the recent ($t_{ej} < 1$ Myr) runaway stars (blue [1]). The mass function of the core population of 5 core collapsed star-cluster simulations is presented in red, which is slightly steeper (power-law slope -1.7) than the runaway mass function, but the measurement was taken just before the first bully binary formed. The mass function within $0.8r_{core}$ is indistinguishable from the runaway mass function. Overplotted (in orange) is a power-law with a slope of -1.5 , the Salpeter (green) mass function (power-law with slope -2.35).

orbital separation of ~ 15.5 au. From 15.5 au down to the observed 3.63 au Mel 34 has liberated about 3000 kT in kinetic energy. This is enough to eject 439 stars of $10 M_{\odot}$, or 3 stars of $100 M_{\odot}$ at 100 km/s. Bear in mind, though, that every time Mel 34 kicks out a star, it also propels itself in the opposite direction.

Appendix C: The role of VFTS590

The encounter that led to the ejection of Mel 34 must conserve linear and angular momentum. If Mel 34 ejected VFTS 590, another object must be ejected along the magenta line in fig. 1 (main paper). There is no prominent candidate star with a measured proper motion along this line up to a distance of ~ 600 pc [1].

If we assume that a $15 M_{\odot}$ star, barely observable at the distance of the LMC, is the star we are looking for; it then was ejected with a velocity of ~ 990 km/s or a kinetic energy of ~ 46500 kT to conserve linear momentum. The binary Mel 34 cannot have achieved this because if another binary participated in this encounter (of which this $15 M_{\odot}$ runaway was a member), its orbital separation would have been smaller than the main-sequence radii of both stars. An encounter can hardly produce such a high velocity but rather result in a collision [31].

Appendix D: The mystery star

We performed 4-body (binary-binary) scattering experiments using starlab [32] to determine the most favorable mass of the unknown runaway. An encounter with both binaries at orbital separations of 2 to 4 au would suffice to eject all objects in their appropriate directions with the observed velocity. It requires the encountering binary, composed of Mel 34A (or Mel 34B) and VFTS 590 in a 2 to 4 au orbit to be broken up, and the primary to exchange for our unknown runaway star. The largest cross-section and the most probably post-encounter parameters are achieved for a $\sim 90 M_{\odot}$ star. Currently this $90 M_{\odot}$ mystery runaway star would be at a distance of about 8.5 pc from the R136's center moving away along the magenta line in figure 1 with a velocity of about 180 km/s; such a star is not observed.

We cannot fully exclude the hypothesis that the VFTS 590 and Mel34AB were ejected through a 4-body encounter in which one of the stars has a mass below the detection limit of $10 M_{\odot}$. In that case the most probable encounter is between a target binary composed of Mel 34A and VFTS 590 in a 2 to 4 au orbit that interacts with the projectile binary composed of Mel 34B and a $< 10 M_{\odot}$ star (below the detection limit). The projectile binary then must have an orbital separation $\lesssim 0.2$ au, in order to accommodate the post-encounter energetics. Note that the cross section for this interaction is almost identical if we swap Mel 34A for Mel 34B.

Such an interaction leads to a runaway velocity for VFTS 590 of 114 ± 71 km/s with a median of ~ 99 km/s, consistent with the observed velocity of 83.4 ± 6.2 km/s. The post-encounter binary Mel 34AB, would then acquire a median velocity of ~ 199 km/s, much higher than the observed 64 km/s. Note that these velocities are acquired under the assumption that all four stars are point-masses: and no collisions can occur. The probability, however, that this interaction leads to a collision between two (or even three) stars is more than 60 times larger than the clean exchange and ionization interaction in which VFTS 590 and Mel 34AB would be ejected. A collision between two or even three of the participating stars will not lead to high-velocity runaways. The data for these calculations are available at Zenodo (<https://zenodo.org/uploads/10256841>).

We do expect that several collisions have occurred in the central portion of R 136, but not in the recent encounter that launched Mel 34AB.

Appendix E: Calculating the interaction cross sections

E.1. Automatic cross section detection

STARLAB has a handy package for the automatic determination of cross sections, called SIGMA3. We expanded SIGMA3 to calculate multi-body cross sections [33]. In SIGMA3, one starts by launching a projectile single star onto a target binary with semi-major axis $a = 1$ (in dimensionless N-body units [34]) in the X-Y plane with the periaapsis along the positive X-axis. The center of mass of the multi-body system was centred on the origin. The single incoming star is initialized at $100a$ from a random direction and an impact parameter that brings it within a of the binary. This process is repeated until the desired surface density of encounters is reached. In our calculations, we adopted a trial density of 10^3 . Suppose one or more encounters lead to anything else than a non-resonant preserving interaction. In that case, the same procedure is repeated, but now the closest approach distance is between a and a larger distance such that the surface area equals the binary surface area. Again 10^3 scattering experiments are performed, and if any of the experiments result in a non-preserving encounter this procedure is repeated until all encounters in the outermost ring result in a preserving encounter.

The cross-section σ is subsequently calculated from the largest impact parameter b for which an encounter leads to any outcome other than a preserving encounter: $\sigma = \pi b^2 \times n_{\text{hit}}/N_{\text{exp}}$. Here N_{exp} is the number of scattering experiments with impact parameter $< b$, and n_{hit} is the number of cases where the experiment resulted in the desired final configuration.

E.2. 3-body scattering

We use SIGMA3 to calculate the 3-body interaction cross-section between a binary and a single star. The three stars, Mel 34A, Mel34B, and VFTS 590, appear in avarious configurations in the target binary and projectile incoming star.

We performed a total of 382104 3-body scattering experiments in order to determine the cross-section for accelerating Mel 34 and VFTS 590 to a minimum velocity of 27.6 km/s. We adopted orbital separations for Mel 34A and Mel 34B between 1 au and 1500 au (in 10 equally separated logarithmic bins), and varied the incoming velocity from 7 km/s to 10 km/s with 1 km/s increments. We conclude that it requires considerable fine-tuning to have VFTS 590 acquire its observed velocity, and preserved angular momentum; the cross-section for this interaction is negligible small.

E.3. 4-body scattering

In four-body scattering experiments, we adopt that either two binaries interact or a triple interacts with a single star. One is considered the target, and the other is the projectile. The cross sections are determined automatically using the procedure set out for 3-body encounters, except that now the projectile may be a binary star with semi-major axis a_p . The package for the 4-body encounter cross-section determination is called SIGMA, and generalizes SIGMA3 [33].

A total of 344288 4-body scattering experiments were conducted for this study. These runs were used to further constrain the most suitable parameters in the case that VFTS 590 would have been a binary companion before encountering Mel 34. The semi-major axis of the target binary was varied between 2 au and 8 au (with constant increments of 1 au), and the projectile binary between 2 au and 18 au (with constant increments of 1 au). The relative encounter velocity was varied between 3 km/s and 18 km/s (with constant increments of 1 km/s).

From these calculations, we conclude that a four-body encounter cannot satisfactorily explain the observed velocities of VFTS 590 and Mel 34, nor the orbital separation of the latter.

E.4. 5-body scattering

The most elaborate and complicated calculations are the 5-body encounters, for which we also use the SIGMA package [33] from STARLAB [32]. For those, we focus on a target triple $((t_{11}, t_{12}), t_2)$ that interacts with a projectile binary (p_1, p_2) .

We performed a total of 1,565,520 5-body scattering experiments distributed over 76 cross-section calculations for a range of initial conditions. With the calculations, we pin-point the choice of initial conditions calibrated for the theoretical arguments set out in main manuscript. These arguments are based on the conservation of energy before and after the dynamical interaction, and the expected amount of energy released in the interaction (see eq. (1)). We further explore, as free parameters, the relative encounter velocity (v_{enc}) between 1 km/s and 13 km/s (see table E.II), and the orbit of the tertiary star (which is ill constrained by the energetics, see table E.III). Once the optimal set of parameters for the pre-encounter configuration of the binary and the triple are found, we performed an extra set of runs to study the sensitivity of the conditions. We performed 76 cross section calculations for 5-body (binary-triple) interactions.

After constraining the parameters for the 5-body encounters, we focus on the interaction between a target triple and a projectile binary. To limit parameter space, we assume that VFTS 590 has a mass of $50 M_\odot$, Mel39B is $80 M_\odot$ and the other stars are $130 M_\odot$. We realize that the slight differences in mass between Mel 34A ($139 M_\odot$), Mel 34B ($127 M_\odot$), and Mel 39A ($140 M_\odot$) are relevant for our calculations, but the simplification helps in acquiring a global understanding of the consequences of the interaction, before constraining the specific masses of Mel34A, Mel34B, and Mel39A, which are rather similar in a dynamical perspective.

After determining the cross sections, we realize scenario G is most promising, as explained in the main text. In order to explore the effect of the incoming relative velocity, we adopt model G and calculate the interaction with a relative velocities of 1 km/s to 13 km/s. The results of these calculations are presented in table E.II.

To illustrate the sensitivity of the orbital separation for the two binaries, we present the results of cross-section calculations for slightly wider systems. We rather arbitrarily adopted 10 au for the inner target binary, 100 au for the orbital separation of the tertiary component, and 10 au for the projectile binary. The resulting cross-sections for the 7 configurations in which we can distribute VTS 590 and Mel39B over the triple and binary are presented in table E.IV.

In figure E.II we present, for model G of table E.IV, the orbital separation and eccentricity for the runaway binaries for Mel 34, Mel 39 after an interaction with initial (pre-encounter) orbital parameters somewhat wider than adopted in the main paper. Comparing figure E.II with figure 3 illustrates the sensitivity of the initial orbital parameters to the relative orbital distributions (in semi-major axis and eccentricity) of the final runaway binaries.

The relative probabilities for the 8 configurations for a triple-binary encounter are presented in table 1. We further specify the interaction by calculating the relative frequency of each of the various branching ratios for the interactions for scenarios A to H (see table E.I in appendix E). The encounters for model G (where VFTS 590 orbiting the target binary) is most probable, leading to a rate of $\sim 27 \text{ Myr}^{-1}$, which is conveniently close to the observed rate of 24 Myr^{-1} [see 1]. The most probable interaction (in model G) is the preservation of both binaries (see table 1).

It may seem that we rather quickly focus on the encounter between a 4 au and 6 au binary, but many parameters were varied to constrain these parameters. We explored the inner target and projectile orbital separation between 2 au and 10 au (with constant increments of 1 au), and the tertiary orbit between 30 au and 320 au (with constant increments of 10 au). The upper limit corresponds to about half the semi-major axis for a hard-soft encounter in the R136's cluster core. The relative velocities were varied between 1 km/s and 13 km/s (with constant increments of 1 km/s). Note that stars with a velocities $> 7 \text{ km/s}$ have escape speed from the cluster core region.

id	escaper	(p ₁ , p ₂)	(p ₁ , t ₁₁)	(p ₁ , t ₂)	(p ₁ , t ₁₂)
(VFTS 590)					
A	t ₂	0	0	–	0
B	t ₂	0.61	0.15	–	0.11
C	p ₂	–	0	0	0
D	t ₁₂	0.75	0.25	0	–
E	t ₂	0	0	–	0
F	t ₁₂	0.54	0.29	0.18	–
G	t ₂	0.83	0.17	–	0.06
H	t ₁₂	0.75	0.17	0.08	–

TABLE E.I. Identification of the escaping star and relative outcome frequency for scenarios A till H for the encounter in which $a_{\text{in}} = 4$ au, $a_{\text{out}} = 40$ au, $a_{\text{projectile}} = 6$ au. For an encounter velocity of $v_{\text{enc}} = 7$ km/s. Scenario G in which t₂ escapes as a single and (p₁, p₂) as well as (t₁₁, t₁₂) escape as binaries give the most probable outcome.

v_{enc}	σ	$f_{\text{esc,VFTS590}}$	σ_{run}	$\Gamma_{\text{esc,VFTS590}}$	(p ₁ , p ₂)	(p ₁ , t ₁₁)	(p ₁ , t ₁₂)
[km/s]	[10 ⁶ au ²]		[10 ⁶ au ²]	[Myr ⁻¹]			
1	34700	0.348	0.053	1840	0.85	0.95	0.05
3	1280	0.383	0.040	156	0.81	0.13	0.06
5	277	0.358	0.028	38.5	0.73	0.18	0.09
7	101	0.323	0.048	33.9	0.83	0.17	0.06
9	47.6	0.340	0.045	19.5	0.72	0.17	0.11
11	26.1	0.340	0.038	10.9	0.73	0.13	0.13
13	15.8	0.365	0.045	9.33	0.94	0.06	0.00

TABLE E.II. Cross section for scenario G but with varying the encounter velocity. Here we adopted the binary (t₁₁, t₁₂) to have a semi-major axis of $a_{\text{in}} = 4$ au. The initial tertiary t₂ (that eventually escapes) orbits the target binary with a semimajor-axis of $a_{\text{out}} = 40$ au. The projectile binary (p₁, p₂), has a semi-major axis of 6 au. The first column gives the relative encounter velocity, followed by the cross section, and the fraction of systems for which VFTS 590 escapes. The following columns give the cross section for VFTS 590 and the two binaries to acquire a minimum runaway velocity of 27.6 km/s, and the encounter rate associated with this cross section. The last three columns give the branching ratios of the eventual surviving binaries with p₁ as primary.

Eventually, we adopt the most opportune result from the relative encounter velocity, and vary the orbital separation of the tertiary star (VFTS 590). The results are presented in table E.III. The orbital separation of the tertiary star has only a minor effect on the interaction cross-section, and on the other final orbital parameters of the two runaway binaries and the velocity of all three runaways. It therefore remains hard to constrain the pre-encounter orbit of VFTS 590 around the binary Mel 39.

Appendix F: The evolution of the runaway binaries

After being ejected from the R136 cluster, the two binaries, Mel 34 and Mel 39, continue to evolve, and Roche-lobe overflow is inevitable for both. We continue their evolution assuming that they were not further perturbed by encounters with other stars. We use the binary evolution code SeBa [35] to estimate the evolution of the two binaries, assuming that they were ejected at an age of 1 Myr, and that they remain unperturbed for the rest of their lifetimes.

Both binaries, Mel 34 and Mel 39 have quite a comparable evolution, which starts with two main-sequence stars in rather tight and elliptic orbits. We illustrate the evolution of both binaries in fig. F.III, and indicate a few key phases by the letters A to D. The shorthand notation, introduced in [35] can be written as

$$\begin{array}{ccccccc} & \text{A} & & \text{B} & & \text{C} & & \text{D} \\ (\text{ms}, \text{ms}) \rightarrow (\text{gs}, \text{ms})_{\text{c}} \rightarrow [\text{gs}, \text{ms}] \rightarrow (\text{WR}, \text{ms}) \rightarrow (\text{bh}, \text{ms}) \rightarrow (\text{bh}, \text{gs})_{\text{c}} \rightarrow \{\text{bh}, \text{gs}\} \rightarrow (\text{bh}, \text{WR}) \rightarrow (\text{bh}, \text{bh}) \rightarrow \{\text{bh}\}. \end{array}$$

The evolution starts with two main sequence stars, indicates as (ms, ms) in elliptic orbits (see lower panel in fig. F.III). In the coming 3 Myr the orbits of both binaries circularizes (indicated with the subscript c), and the stellar winds causes the orbits to widen. The primary star (indicated in the left hand side) ascends the giant branch (gs) just before its hydrogen envelope runs out, and fills it's Roche lobe (indicated in fig. F.III with the vertical dashed line and the letter A). Mass transfer from the primary star (The Roche-lobe filling star is indicated in the short-hand notation with the square bracket) to the secondary. The primary, being

a_{out}	σ	$f_{\text{esc,VFTS590}}$	σ_{run}	$\Gamma_{\text{esc,VFTS590}}$	$(\mathbf{p}_1, \mathbf{p}_2)$	$(\mathbf{p}_1, \mathbf{t}_{11})$	$(\mathbf{p}_1, \mathbf{t}_{12})$
					$(\mathbf{t}_{11}, \mathbf{t}_{12})$	$(\mathbf{p}_2, \mathbf{t}_{12})$	$(\mathbf{p}_2, \mathbf{t}_{11})$
[au]	$[10^6 \text{ au}^2]$	$[\text{au}^2]$	$[\text{au}^2]$	$[\text{Myr}]^{-1}$			
40	103	0.43	0.046	34	0.83	0.17	0.06
50	142	0.42	0.043	43	0.77	0.09	0.14
60	140	0.43	0.040	39	0.80	0.11	0.10
80	99	0.28	0.033	23	0.75	0.16	0.09
100	135	0.45	0.043	41	0.73	0.14	0.13
120	95	0.56	0.049	33	0.72	0.14	0.13
140	134	0.51	0.042	39	0.77	0.12	0.11
160	133	0.28	0.026	24	0.81	0.06	0.13
180	132	0.65	0.038	36	0.83	0.08	0.09
200	132	0.68	0.039	36	0.75	0.10	0.15
240	132	0.80	0.023	21	0.75	0.13	0.12

TABLE E.III. Branching ratios and cross-section for scenario G (t_2 escapes) for the varying orbit of the tertiary star (VFTS 590) around the inner binary (t_{11}, t_{12}). The inner target binary has an adopted semi-major axis of 4 au, while the projectile binary has a semi-major axis of 6 au. The relative encounter velocity is 7 km/s. The first column gives the semi-major axis of the tertiary star (t_2) around the target binary (t_{11}, t_{12}). The following column gives the cross section for this interaction to happen. The next three columns give the fraction of systems, cross-section and the rate for the escaper (VFTS 590) to acquire a runaway speed of at least 27.6 km/s. The last three columns give the branching ratios of the eventual surviving binaries with p_1 as primary.

id	Encounter	σ	$f_{\text{esc,VFTS590}}$	f_{run}	$\Gamma_{\text{esc,VFTS590}}$
		$[10^6 \text{ au}^2]$	$[\text{au}^2]$		$[\text{Myr}]^{-1}$
A	$\langle((t_{11}, t_{12}), t_2), (\text{Mel39B}, \text{VFTS 590})\rangle$	132	0.003	0.000	0.00
B	$\langle((t_{11}, t_{12}), \text{VFTS 590}), (p_1, \text{Mel39B})\rangle$	144	0.502	0.008	7.56
C	$\langle((t_{11}, t_{12}), \text{Mel39B}), (p_1, \text{VFTS 590})\rangle$	134	0.001	0.000	1.25
D	$\langle((t_{11}, \text{VFTS 590}), t_2), (p_1, \text{Mel39B})\rangle$	231	0.174	0.002	284
E	$\langle((t_{11}, \text{Mel39B}), t_2), (p_1, \text{VFTS 590})\rangle$	148	0.002	0.000	1.62
F	$\langle((t_{11}, \text{VFTS 590}), \text{Mel39B}), (p_1, p_2)\rangle$	290	0.128	0.003	263
G	$\langle((t_{11}, \text{Mel39B}), \text{VFTS 590}), (p_1, p_2)\rangle$	281	0.492	0.042	977
H	$\langle((\text{Mel39B}, \text{VFTS 590}), t_2), (p_1, p_2)\rangle$	296	0.141	0.004	296

TABLE E.IV. Cross sections for the 8 reduced cases for which we adopt Mel39B as a $80 M_{\odot}$ star, and $50 M_{\odot}$ for VFTS 590. All the other stars are $140 M_{\odot}$. Calculations are performed with a semi-major axis for the inner target binary of $a = 10$ au and an outer orbit of 100 au. For the projectile binary, we also adopt 10 au. The relative encounter velocity is $v_{\text{enc}} = 7$ km/s. The first column identifies the scenario, explains the second column. The third and fourth columns give the total cross section for this interaction and the fraction of cases in which VFTS 590 is ejected. The last two columns give the cross-section and rate for VFTS 590 to be ejected with a velocity of at least 27.6 km/s.

stripped of it's envelope, becomes a naked helium star (WR) and collapses a some time later to a black hole (bh, indicated with the letter B in fig. F.III). The first supernovae in Mel 34 and Mel 39 occur around the same time, and for clarity, is only indicated in blue in fig. F.III. The secondary star subsequently, ascends the giant branch, circularizes the orbit, and commences into a common envelope (indicated with braces, and the letter C in fig. F.III). The resulting tight binary is composed of the primary black hole and the stripped core of the Roche-lobe filling giant. The resulting Wolf-Rayet star collapses into a black hole in a supernova (indicated by the letter D in fig. F.III). If the binary survives (here we neglected natal kicks in the supernova, allowing both binaries to survive the mass loss in the supernovae) the two black holes eventually merge into a single black hole due to the emission of gravitational waves.

The orbital separation of the two black hole binaries, however, is too large, and their eccentricities too small to make the black holes merge in a Hubble time due to the emission of gravitational waves.

ENERGY CONSUMPTION OF THIS CALCULATION

In the spirit of the energy consumption of our scientific endeavour [36], we report on our energy consumption for the calculations in this research. The calculations using STARLAB and AMUSE took about $2.9 \cdot 10^7$ core seconds. Runs are performed on

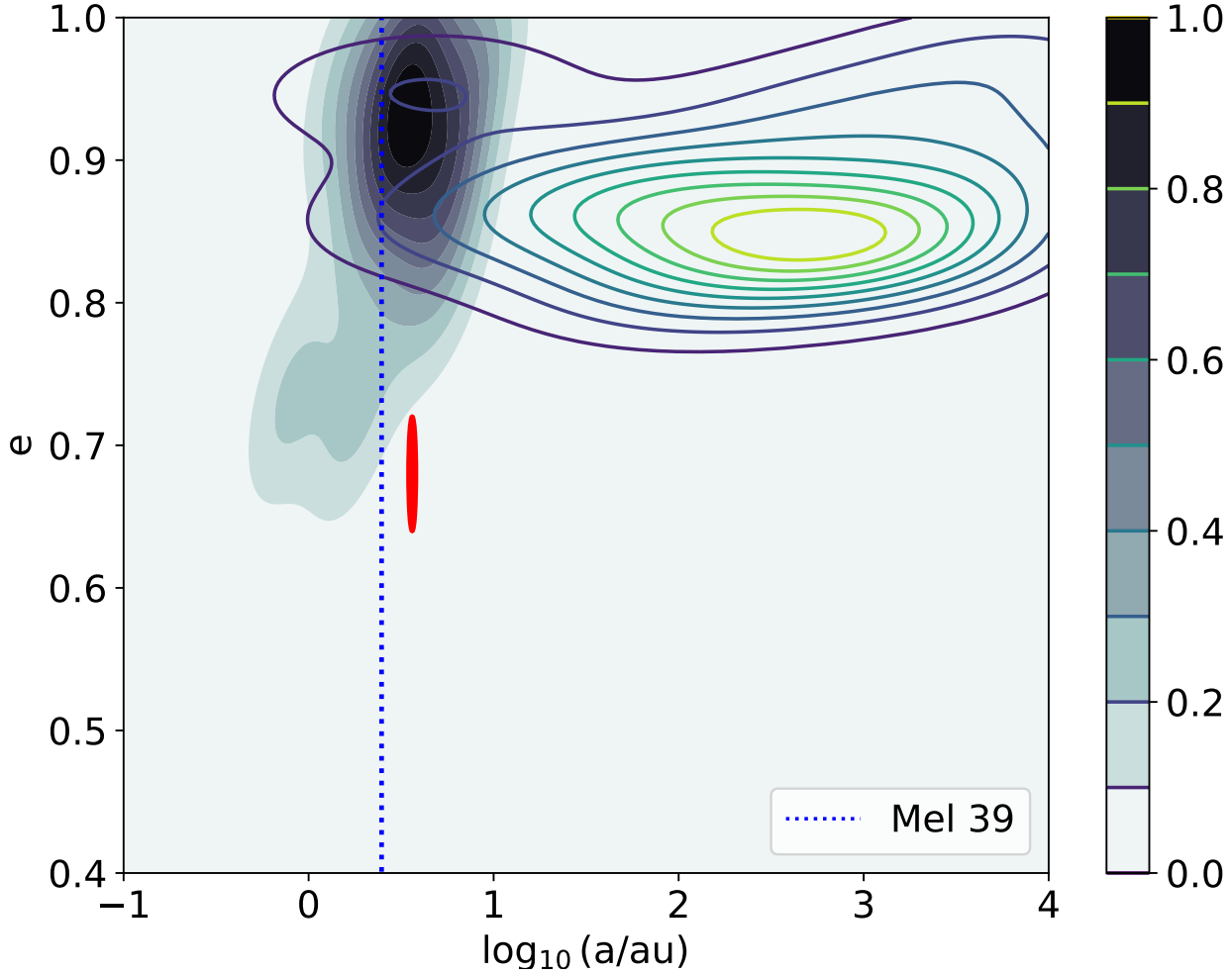


FIG. E.II. Orbital separation vs eccentricity for scenario G in which Mel 34 (grey shades, color bar to the right) and Mel 39 (contours, overplotted in the right-hand color bar) for an interaction in which the inner target and the projectile binaries have an orbital separation of 10 au, whereas the tertiary star (VFTS 590) is 100 au. Note the four-times wider range in the x-axis compared to fig. 3. The red ellipsoid point gives the observed orbital parameters for Mel 34 (its size is 4 standard deviations, twice the range as in fig. 3), and the vertical blue dotted line gives the observed semi-major axis (assuming an $80 M_{\odot}$ star for the secondary) for Mel 39.

a 165 Watt 12-core Xeon E-2176M CPU with NVIDIA Quadro P1000 Max-Q GPU, totaling about 110 KWh. The origin of the electricity was wind and solar.

* spz@astronomy.nl

† Also at Institute of Astronomy, KU Leuven, Celestijnenlaan 200 D, Leuven, 3001, Belgium.

- [1] M. Stoop, A. de Koter, L. Kaper, S. Brands, S. Portegies Zwart, H. Sana, F. Stoppa, M. Gieles, L. Mahy, T. Shenar, D. Guo, G. Nelemans, S. Rieder, Two waves of massive stars running away from the young cluster R136, *Nat* 634 (8035) (2024) 809–812. [arXiv:2410.06255](#), [doi:10.1038/s41586-024-08013-8](#).
- [2] A. Blaauw, On the origin of the O- and B-type stars with high velocities (the "run-away" stars), and some related problems, *Bul. Astron. Inst. Neth.* 15 (1961) 265–.
- [3] J. Boersma, Mathematical theory of the two-body problem with one of the masses decreasing with time, *Bul. Astron. Inst. Neth.* 15 (1961) 291–301.
- [4] J. G. Hills, The effects of sudden mass loss and a random kick velocity produced in a supernova explosion on the dynamics of a binary star of arbitrary orbital eccentricity - Applications to X-ray binaries and to the binary pulsars, *ApJ* 267 (1983) 322–333. [doi:10.1086/160871](#).

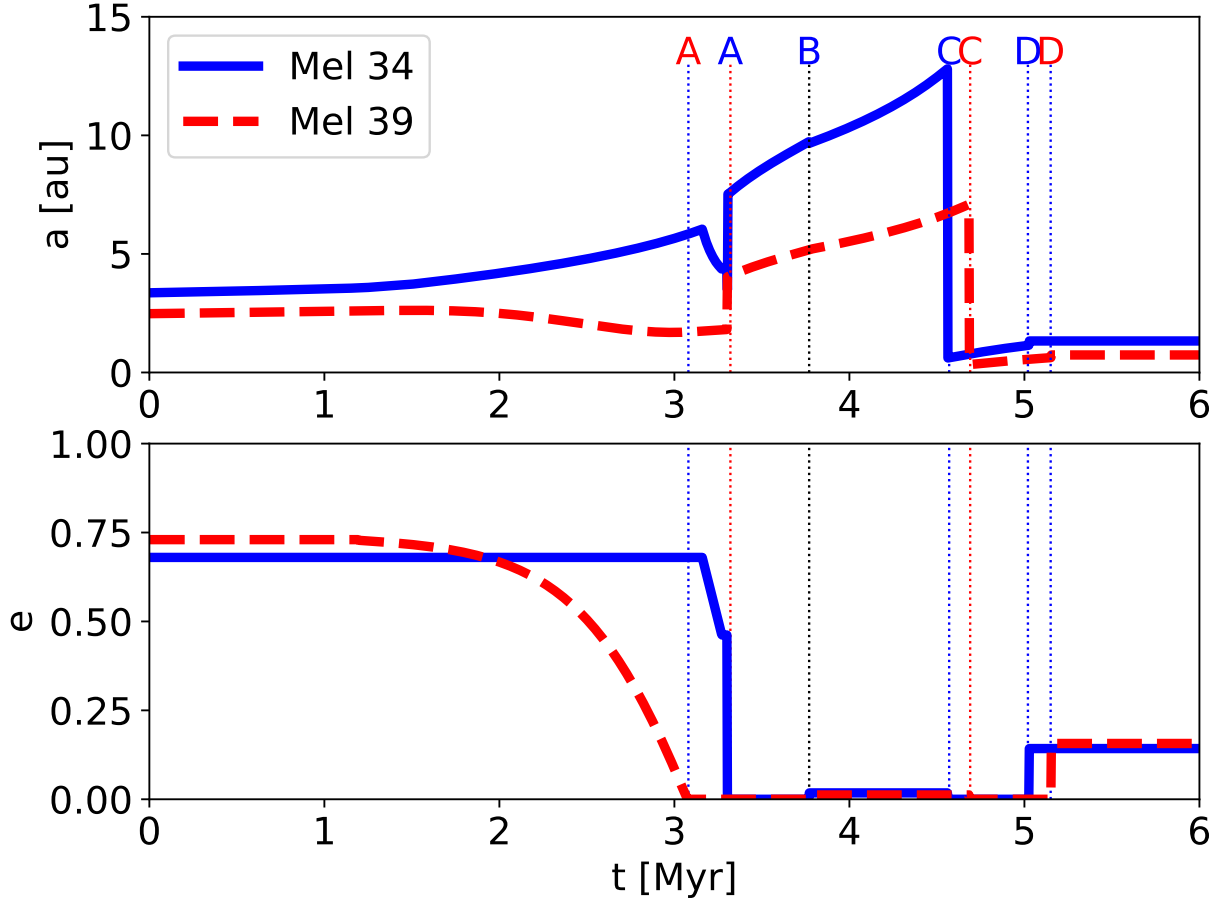


FIG. F.III. Orbital evolution of the two binaries Mel 34 (blue) and Mel 39 (red) after they have been ejected from the star cluster R136. The top panel shows the evolution of the orbital separation, the bottom panel shows the eccentricity. We identify 4 distinct events in the binary evolution, which are A: the onset of mass transfer, B: the first supernova, C: the initiation of the second phase of mass transfer, and D: the second supernova at about 6 Myr (after which we stop the calculation). The letters correspond to the short-hand notation presented in the text. Both binaries remain bound afterwards, but eventually (after many Hubble times) will merge due to the emission of gravitational waves.

- [5] M. S. Fujii, S. Portegies Zwart, The Origin of OB Runaway Stars, *Science* 334 (2011) 1380–. [arXiv:1111.3644](#), [doi:10.1126/science.1211927](#).
- [6] S. F. Portegies Zwart, S. L. W. McMillan, M. Gieles, Young Massive Star Clusters, *ARA&A* 48 (2010) 431–493. [arXiv:1002.1961](#), [doi:10.1146/annurev-astro-081309-130834](#).
- [7] P. A. Crowther, O. Schnurr, R. Hirschi, N. Yusof, R. J. Parker, S. P. Goodwin, H. A. Kassim, The R136 star cluster hosts several stars whose individual masses greatly exceed the accepted $150M_{\text{stellar}}$ stellar mass limit, *MNRAS* 408 (2) (2010) 731–751. [arXiv:1007.3284](#), [doi:10.1111/j.1365-2966.2010.17167.x](#).
- [8] S. A. Brands, A. de Koter, J. M. Bestenlehner, P. A. Crowther, J. O. Sundqvist, J. Puls, S. M. Caballero-Nieves, M. Abdul-Masih, F. A. Driessen, M. García, S. Geen, G. Gräfener, C. Hawcroft, L. Kaper, Z. Keszthelyi, N. Langer, H. Sana, F. R. N. Schneider, T. Shenar, J. S. Vink, The R136 star cluster dissected with Hubble Space Telescope/STIS. III. The most massive stars and their clumped winds, *A&A* 663 (2022) A36. [arXiv:2202.11080](#), [doi:10.1051/0004-6361/202142742](#).
- [9] S. F. Portegies Zwart, E. P. J. van den Heuvel, A runaway collision in a young star cluster as the origin of the brightest supernova, *Nat* 450 (2007) 388–389. [arXiv:arXiv:0711.2293](#), [doi:10.1038/nature06276](#).
- [10] A. Blaauw, W. W. Morgan, The space motions of α aurigae and μ columbae with respect to the orion nebula., *ApJ* 119 (1954) 625.
- [11] A. Poveda, J. Ruiz, C. Allen, *Boletín de los Observatorios de Tonantzintla y Tacubaya*.
- [12] B. Polak, M.-M. Mac Low, R. S. Klessen, S. Portegies Zwart, E. P. Andersson, S. M. Appel, C. Cournoyer-Cloutier, S. C. O. Glover, S. L. W. McMillan, Massive star cluster formation: II. Runaway stars as fossils of subcluster mergers, *A&A* 690 (2024) A207. [arXiv:2405.12286](#), [doi:10.1051/0004-6361/202450774](#).

- [13] K. A. Tehrani, P. A. Crowther, J. M. Bestenlehner, S. P. Littlefair, A. M. T. Pollock, R. J. Parker, O. Schnurr, Weighing Melnick 34: the most massive binary system known, *MNRAS* 484 (2) (2019) 2692–2710. [arXiv:1901.04769](#), [doi:10.1093/mnras/stz147](#).
- [14] S. F. Portegies Zwart, S. L. W. McMillan, Gravitational thermodynamics and black-hole mergers, *Int. J. of Mod. Phys. A* 15 (2000) 4871–4875. [doi:10.1142/S0217751X00002135](#).
URL <http://journals.wspc.com.sg/139/15/1530/S0217751X00002135.html>
- [15] D. C. Heggie, Binary evolution in stellar dynamics, *MNRAS* 173 (1975) 729–787.
- [16] D. Heggie, P. Hut, The Gravitational Million-Body Problem: A Multidisciplinary Approach to Star Cluster Dynamics, *The Gravitational Million-Body Problem: A Multidisciplinary Approach to Star Cluster Dynamics*, by Douglas Heggie and Piet Hut. Cambridge University Press, 2003, 372 pp., 2003.
- [17] P. Hut, S. McMillan, R. W. Romani, The evolution of a primordial binary population in a globular cluster, *ApJ* 389 (1992) 527–545.
- [18] S. F. Portegies Zwart, S. L. W. McMillan, The Runaway Growth of Intermediate-Mass Black Holes in Dense Star Clusters, *ApJ* 576 (2002) 899–907. [arXiv:astro-ph/0201055](#), [doi:10.1086/341798](#).
- [19] J. M. Bestenlehner, P. A. Crowther, S. M. Caballero-Nieves, F. R. N. Schneider, S. Simón-Díaz, S. A. Brands, A. de Koter, G. Gräfener, A. Herrero, N. Langer, D. J. Lennon, J. Maíz Apellániz, J. Puls, J. S. Vink, The R136 star cluster dissected with Hubble Space Telescope/STIS - II. Physical properties of the most massive stars in R136, *MNRAS* 499 (2) (2020) 1918–1936. [arXiv:2009.05136](#), [doi:10.1093/mnras/staa2801](#).
- [20] A. M. T. Pollock, P. A. Crowther, J. M. Bestenlehner, P. S. Broos, L. K. Townsley, Melnick 39 is a very massive intermediate-period colliding-wind binary, *MNRAS* 539 (2) (2025) 1291–1298. [arXiv:2503.17150](#), [doi:10.1093/mnras/staf501](#).
- [21] R. A. Mardling, S. J. Aarseth, Tidal interactions in star cluster simulations, *MNRAS* 321 (2001) 398–420.
- [22] J.-P. Zahn, Tidal friction in close binary stars, *A&A* 57 (1977) 383–394.
- [23] P. Massey, L. R. Penny, J. Vukovich, Orbits of Four Very Massive Binaries in the R136 Cluster, *ApJ* 565 (2002) 982–993. [arXiv:arXiv:astro-ph/0110088](#), [doi:10.1086/324783](#).
- [24] B. P. Abbott, et al., Kagra Collaboration, VIRGO Collaboration, Prospects for observing and localizing gravitational-wave transients with Advanced LIGO, Advanced Virgo and KAGRA, *Living Reviews in Relativity* 21 (1) (2018) 3. [arXiv:1304.0670](#), [doi:10.1007/s41114-018-0012-9](#).
- [25] S. Portegies Zwart, S. McMillan, *Astrophysical Recipes*, 2514-3433, IOP Publishing, 2018. [doi:10.1088/978-0-7503-1320-9](#).
URL <http://dx.doi.org/10.1088/978-0-7503-1320-9>
- [26] E. E. Salpeter, The luminosity function and stellar evolution., *ApJ* 121 (1955) 161.
- [27] H. C. Plummer, On the problem of distribution in globular star clusters, *MNRAS* 71 (1911) 460–470.
- [28] D. P. Caputo, N. de Vries, S. Portegies Zwart, On the effects of subvirial initial conditions and the birth temperature of R136, *MNRAS* 445 (1) (2014) 674–685. [arXiv:1409.4765](#), [doi:10.1093/mnras/stu1769](#).
- [29] I. R. King, The structure of star clusters. iii. some simple dvriamical models, *AJ* 71 (1966) 64–75.
- [30] J. Makino, P. Hut, On core collapse, *ApJ* 383 (1991) 181–191. [doi:10.1086/170774](#).
- [31] V. V. Gvaramadze, A. Gualandris, S. Portegies Zwart, On the origin of high-velocity runaway stars, *MNRAS* 396 (2009) 570–578. [arXiv:0903.0738](#), [doi:10.1111/j.1365-2966.2009.14809.x](#).
- [32] S. F. Portegies Zwart, P. Hut, S. L. W. McMillan, J. Makino, Star cluster ecology - V. Dissection of an open star cluster: spectroscopy, *MNRAS* 351 (2004) 473–486. [arXiv:arXiv:astro-ph/0301041](#), [doi:10.1111/j.1365-2966.2004.07709.x](#).
- [33] A. Gualandris, S. Portegies Zwart, P. P. Eggleton, N-body simulations of stars escaping from the Orion nebula, *MNRAS* 350 (2004) 615–626. [arXiv:arXiv:astro-ph/0401451](#), [doi:10.1111/j.1365-2966.2004.07673.x](#).
- [34] D. C. Heggie, R. D. Mathieu, Standardised Units and Time Scales, in: P. Hut, S. L. W. McMillan (Eds.), *The Use of Supercomputers in Stellar Dynamics*, Vol. 267 of Lecture Notes in Physics, Berlin Springer Verlag, 1986, p. 233. [doi:10.1007/BFb0116419](#).
- [35] S. F. Portegies Zwart, F. Verbunt, Population synthesis of high-mass binaries., *A&A* 309 (1996) 179–196.
- [36] S. Portegies Zwart, The ecological impact of high-performance computing in astrophysics, *Nature Astronomy* 4 (2020) 819–822. [arXiv:2009.11295](#), [doi:10.1038/s41550-020-1208-y](#).